JMBFS
Journal of Microbiology, Biotechnology and Food Sciences
International peer-reviewed scientific online journal
Published by Faculty of Biotechnology and Food Sciences

SUNLIGHT-DRIVEN INSTANT SYNTHESIS OF SILVER NANOPARTICLES USING AQUEOUS FRUIT EXTRACT OF *TERMINALIA PANICULATA* ROTH AND *IN VITRO* ASSESSMENT OF ITS ANTIOXIDANT AND ANTI-INFLAMMATORY ACTIVITIES

Nirupa S. Vernekar[1], Tarikere C. Taranath[1]*

Address(es):
[1]Environmental Biology and Green Nanotechnology Laboratory, P. G. Department of Studies in Botany, Karnatak University, Dharwad – 580003, Karnataka, India.

*Corresponding author: tctaranath@gmail.com

https://doi.org/10.55251/jmbfs.9236

ARTICLE INFO

Received 22. 7. 2022
Revised 10. 5. 2023
Accepted 11. 5. 2023
Published 1. 8. 2023

Regular article

OPEN ACCESS

ABSTRACT

Herein we report a sunlight-driven, instant, one-step, green route for the synthesis of silver nanoparticles (AgNPs) using aqueous fruit extract of *Terminalia paniculata* Roth and *in vitro* assessment of its antioxidant and anti-inflammatory activities. 5 mL of aqueous fruit extract of *T. paniculata* was added to 95 mL of 1 mM $AgNO_3$ and exposed to direct sunlight. The *T. paniculata* fruit extract mediated AgNPs (TpF-AgNPs) were characterized for their morphological, physical, and chemical properties using UV-Vis Spectroscopy, Fourier-Transform Infrared Spectroscopy (FTIR), X-Ray Diffraction (XRD), Dynamic Light Scattering (DLS), Atomic Force Microscopy (AFM) and High-Resolution Transmission Electron Microscopy (HR-TEM) with Selected Area Electron Diffraction (SAED). The antioxidant activity of TpF-AgNPs was evaluated using DPPH (2,2-diphenyl-1-picrylhydrazyl) free radical scavenging assay and the anti-inflammatory activity by Bovine Serum Albumin (BSA) anti-denaturation assay at different doses. The formation of TpF-AgNPs was observed as a colour change from pale-yellow to reddish-brown within 3 mins under direct sunlight. UV-Vis spectra revealed an absorption peak at 411 nm, which is the characteristic for silver nanoparticles. FTIR spectra revealed the possible functional groups of phytochemicals such as -OH and -NH involved in the reduction and capping of TpF-AgNPs. HR-TEM analysis confirmed the spherical shape of nanoparticles with sizes ranging from 5-50 nm with an average particle size of 26 nm. AFM shows surface topography of TpF-AgNPs. The crystalline nature with Face Centered Cubic structure was confirmed through XRD and SAED. The negative value of zeta potential (-53.9 mV) indicated the excellent stability of nanoparticles. The TpF-AgNPs exhibited maximum % scavenging of 71.72 ± 0.51 at 100 µg/mL for antioxidant activity and maximum % inhibition of 85.88 ± 1.09 at 500 µg/mL for anti-inflammatory activity. The sunlight-driven green synthesis of TpF-AgNPs proved to be an instant method in the formation of small-sized nanoparticles exhibiting good antioxidant and anti-inflammatory activity.

Keywords: Green Synthesis, Phytochemicals, Zeta Potential, HR-TEM, Protein Anti-denaturation

INTRODUCTION

Nanotechnology has recently evolved as the cutting-edge technology with myriad biomedical applications. "Nanotechnology is the science that deals with matter at the scale of 1 billionth of a meter (i.e., 10^{-9} m = 1 nm)." **(Horikoshi and Serpone, 2013)**. A nanoparticle is a tiny microscopic particle with atleast one dimension less than 100 nm in size. Conventionally, nanoparticles were synthesized using physical and chemical methods, but these methods make use of toxic chemicals, require high temperature, pressure, are time consuming, and expensive. So, it is the need of the hour to switch on to green synthesis of nanoparticles that is safe, easy, cost-efficient, environmentally-benign technique, free from harmful by-products, and safe for biomedical applications **(Chaudhuri and Malodia, 2017; Hashemi *et al.*, 2016; Herlekar *et al.*, 2014).**

Plants have been an excellent source of bioactive compounds. Since time immemorial, humans have relied on plants as a source of traditional medicine and have included them as a habitual treatment for several diseases **(Rios and Recio, 2005)**. Among various biological entities, plants have come up as nanofactories in the synthesis of nanoparticles **(Ahmed and Ikram, 2015)**. Using plants over micro-organisms helps in reducing the tedious process of maintaining cell cultures and multiple purification steps **(Chaudhuri and Malodia, 2017)**. The synthesis of nanoparticles using plant extract as the reducing agent and sunlight as the catalyst is in the limelight as the process is sustainable, cost-efficient and benign. The phytochemicals of plant extracts get photosensitized on exposure to sunlight and result in electron transfer that reduce silver ions to silver nanoparticles. In addition, phytochemicals act as capping agents, which help in stabilization and prevent agglomeration of nanoparticles **(Venkatasubbaiah *et al.*, 2021)**. A number of reports using plant extracts such as of *Durio zibethinus* **(Sumitha *et al.*, 2018a)**, *Premna integrifolia* **(Singh *et al.*, 2019)**, *Sida retusa* **(Sooraj *et al.*, 2021)**, *Annona squamosa* **(Jose *et al.*, 2021)** etc., have demonstrated synthesis of AgNPs under sunlight. For ages, silver has been extensively known for its anti-microbial properties, and is an attractive nanomaterial compared to other metals in the field of nanotechnology **(Sivamaruthi *et al.*, 2019)**.

During the process of mitochondrial oxidative phosphorylation, reactive oxygen species (ROS) such as hydrogen peroxide (H_2O_2), hydroxyl radical ($HO^{\cdot}$), superoxide anion radical (O_2^{-}) are generated by the partial reduction of oxygen. Moderate levels of ROS play an important role in regulating the physiology of the cell such as cell growth, transduction of cell signaling, and defense against pathogens. But when the level of ROS increases or cellular antioxidant capacity decreases, a condition called oxidative stress occurs, which leads to the damage of nucleic acids, proteins, and lipids **(Ray *et al.*, 2012; Valko *et al.*, 2007)**. This in turn leads to inflammation, cardiovascular diseases, diabetes, degenerative diseases, and cancer **(Cai *et al.*, 2004)**. Inflammation is a bodily protective response to inactivate or destroy the invading organisms, or to remove any irritants that cause tissue injury, infection, or destruction characterized by heat, redness, pain, swelling in the affected area, and disturbed physiological functions. This is due to the chemical mediators released from injured tissue **(Chandra *et al.*, 2012)**. During inflammation, vascular permeability and protein denaturation increases, and alteration of the membrane takes place **(Narayana and Chitra, 2018)**.

For relieving oxidative stress, there are several synthetic antioxidative supplements available such as butylated hydroxyanisole and butylated hydroxytoluene, but they are expensive and have side effects like carcinogenesis **(Botterweck *et al.*, 2000)**. Similarly, to manage inflammation there are non-steroidal anti-inflammatory drugs (NSAIDs) but they also have side effects like the formation of gastric ulcers **(Tripathi, 2008)**. The source of natural antioxidants are phenols and flavonoids, which are found in plants and are less expensive, free from side effects and also act as excellent anti-inflammatory agents **(Ravipati *et al.*, 2012)**. Many researchers have recently focused on developing new drugs from plant sources based on nanotechnology that are of low-cost and effective **(Mohamed El-Rafie and Abdel-Aziz hamed, 2014)**.

The plant *Terminalia paniculata* Roth commonly known as kindal tree belongs to the Combretaceae family. It is a tropical deciduous tree with large natural distribution in the Western Ghats of India. In traditional medicine, the bark and flower juice are used in the treatment of cholera, menstrual disorders, and inflamed parotid glands **(Talwar *et al.*, 2011)**. The fruits are rich in tannins and are used in

dyeing **(Aswathi and Ernest Thoppil, 2020)**. The members of genus *Terminalia* have been widely used in most parts of the world as a source of traditional medicine in treating various diseases **(Eloff *et al*., 2008)** and have been used for several biomedical applications but *T. paniculata* remains unexplored for its therapeutic use.

The main objective of the present study was to establish a sunlight-driven, instant, one-step, green route for the synthesis of silver nanoparticles (AgNPs) using the aqueous fruit extract of *Terminalia paniculata* Roth and to assess its *in vitro* antioxidant and anti-inflammatory activities. To the best of our knowledge, there are no reports to date on the same line of work.

MATERIALS AND METHODS

Chemicals and Glasswares

All the chemicals used for the study were of analytical (AR) grade. DPPH (2,2-diphenyl-1-picrylhydrazyl) from Sigma-Aldrich, Silver Nitrate ($AgNO_3$), and BSA (Bovine Serum Albumin) were purchased from HiMedia Laboratories Pvt. Ltd. and used without further purification. The glasswares were cleaned, sterilized, and dried in a hot air oven before use.

Sample Collection

Healthy fruits of *Terminalia paniculata* Roth used for the study were collected in December 2021 from the campus of Karnatak University, Dharwad, Karnataka, India. The plant was identified and authenticated (Acc. No. 19557) by Dr. K. Kotresha, Associate Professor, Karnatak Science College, Dharwad.

Preparation of Aqueous Fruit Extract

The fruits of *T. paniculata* were brought to the laboratory in sealed polythene bags and thoroughly washed under tap water followed by distilled water to remove any dust particles adhered to it. They were shade dried at room temperature to get rid of the residual moisture. Approximately, 10 gms of fruits were added to a conical flask containing 100 mL distilled water and incubated in a water bath at 60-70ºC for about 45 minutes. The extract was allowed to cool down to room temperature, filtered through No. 1 Whatman filter paper, and stored in a refrigerator at 4ºC for future experiments.

Sunlight-Driven Green Synthesis of TpF-AgNPs

5 mL of aqueous fruit extract of *T. paniculata* was added to 95 mL of 1 mM $AgNO_3$ and exposed to direct sunlight. A similar setup was kept at room temperature, and in dark conditions. After the colour change, pH was adjusted to 8. The solution was centrifuged at 13,000 rpm for 30 mins. The pellet obtained was washed thrice with distilled water to get rid of bio-inorganic molecules. It was then dried in a hot air oven and used for further characterization studies and to assess biological activities.

Characterization of TpF-AgNPs

The absorbance of the reaction mixture after the reduction of Ag^+ ions to Ag^0 was measured using UV-Vis double beam Spectrophotometer (Jasco V-670) in the range of 300-600 nm. The functional groups of phytochemicals present in the fruit extract involved in the reduction and capping of TpF-AgNPs were identified using FTIR (Nicolet 6700, Thermo-Fischer Scientific) with the scanning range of 4000 to 400 cm^{-1}. The crystalline nature and size of the TpF-AgNPs were recorded using XRD (RIGAKU Smartlab SE) with 40 kV and a current of 30 mA with Cu Kα (1.5405A˚) radiation and also through SAED analysis. The particle size distribution and zeta potential were studied using a DLS particle size analyzer (HORIBA SZ-100) with the scattering angle set at 90° and the temperature of the holder was 25.0 °C. The shape, size, and distribution of TpF-AgNPs were studied using AFM (Nanosurf easyscan2 AFM) and HR-TEM (Jeol/JEM 2100).

Biological Activities

In vitro Assessment of Antioxidant Activity

DPPH Free Radical Scavenging Assay

The DPPH (2,2-diphenyl-1-picrylhydrazyl) free radical scavenging activity of TpF-AgNPs was performed according to the method reported by **Blois (1958)** with slight modifications. 1 mL of samples (AgNPs/fruit extract) at various concentrations (20, 40, 60, 80, 100 µg/mL) were allowed to react with 1 mL of 0.1 mM DPPH in methanol and incubated in dark for 30 mins. DPPH without sample was taken as control. After incubation, absorbance was measured at 517 nm. Ascorbic acid was used as a standard drug. The % Scavenging was calculated using the following formula.

$$\% \text{ Scavenging} = [(Ac - As)/Ac] \times 100$$

Where Ac stands for the absorbance of the control, and As for absorbance of the sample.

In vitro Assessment of Anti-inflammatory Activity

BSA Protein Anti-denaturation Assay

The BSA protein anti-denaturation assay of TpF-AgNPs was performed according to the method reported by **Grant *et al*., (1970)** and **Aware *et al*., (2017)** with slight modifications. 1 mL of samples (AgNPs/fruit extract) at various concentrations (100, 200, 300, 400, 500 µg/mL) were allowed to react with 1 mL of BSA solution (1% BSA in 50 mM Tris buffer, pH 6.5). BSA without sample was taken as control. The reaction mixture was incubated at room temperature (37ºC) for 20 mins followed by heating in a water bath at 64ºC for 5-10 mins till turbidity develops. On cooling, the absorbance was recorded at 660 nm spectrophotometrically. Diclofenac Sodium was used as a standard drug. The % Inhibition of protein denaturation was calculated using the following formula.

$$\% \text{ Inhibition} = [(Ac - As)/ Ac] \times 100$$

Where Ac stands for absorbance of the control, and As stands for absorbance of the sample.

Statistical Analysis

The tests were performed in triplicates. All the values are expressed as mean ± standard deviation. The data was analysed using one-way analysis of variance (ANOVA) followed by post-hoc Tukey's test and $p < 0.05$ was considered statistically significant.

RESULTS

Visual Observation

The preliminary identification of TpF-AgNPs formation was visualized as a transition in the colour of the reaction mixture after the addition of fruit extract to $AgNO_3$ solution. Under direct sunlight, the colour changed from pale-yellow to reddish-brown within 3 mins (Figure 1). Similar colour inference with 20 mins reaction time was observed at room temperature. Whereas, the setup kept under dark conditions failed to attain the same degree of colour even after hours.

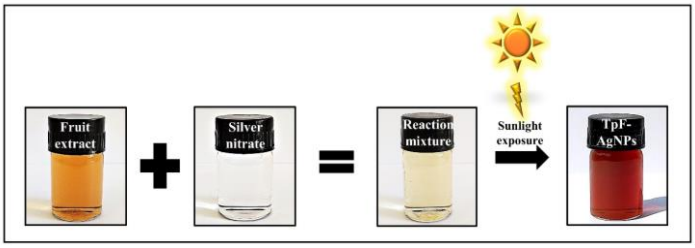

Figure 1 Schematic illustration of TpF-AgNPs formation under direct sunlight.

UV-Vis Spectral Analysis

The reduction of Ag^+ ions to Ag^0 as a change in colour of the reaction mixture was analyzed using UV-Vis Spectroscopy. From figure 2, it can be observed that λmax value after the change in colour of the reaction mixture (pH 4.3) was found to be at 420 nm and it shifted towards 411 nm on adjusting the pH to 8.

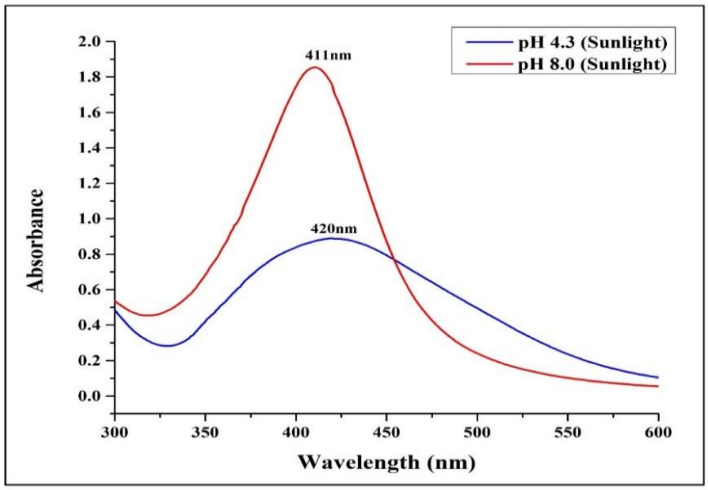

Figure 2 UV-Vis absorption spectra of TpF-AgNPs under direct sunlight (before and after adjusting the pH to 8)

FTIR Spectral Analysis

The FTIR analysis was carried out to study the involvement of phytochemicals of fruit extract in the reduction, capping, and stabilization of TpF-AgNPs. The FTIR spectra of *T. paniculata* fruit extract and *T. paniculata* fruit extract mediated AgNPs are depicted in figure 3. The spectra shows bands at 3399, 2927, 2852, 1733, 1619, 1450, 1357, 1184, 1055, 870, 777, 593 cm^{-1} for fruit extract, and 3424, 2922, 2852, 1617, 1384, 1020 cm^{-1} for TpF-AgNPs respectively. The peak at 3424 cm^{-1} corresponds to -OH stretching vibrations of alcohols and phenols **(Sagadevan *et al*., 2019)**. Peaks at 2922 and 2852 cm^{-1} are attributed to asymmetrical and symmetrical -CH stretching vibrations of alkanes **(Ng S *et al*., 2014; Patil *et al*., 2017)**. A peak at 1617 cm^{-1} was due to the C=C stretching of alkenes **(Mohankumar *et al*., 2012)** and N-H bend in primary amines **(Patil *et al*., 2017)**. The peak at 1384 cm^{-1} could be attributed to the residual amount of $AgNO_3$ **(Abo-Elmagd *et al*., 2020)**. The peak at 1020 cm^{-1} was due to the vibration of the single bond between carbon and nitrogen (C-N) which can be assigned to primary aliphatic amines **(Badmus *et al*., 2020)**.

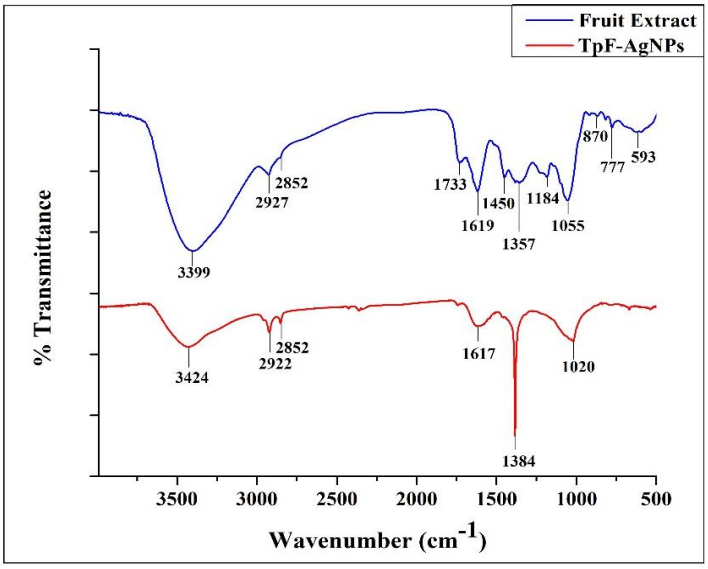

Figure 3 FTIR spectra of *T. paniculata* fruit extract and TpF-AgNPs

XRD Analysis

The crystalline nature of TpF-AgNPs was studied using Powder X-Ray Diffraction (PXRD). The XRD pattern of TpF-AgNPs (Figure 4) shows five distinct peaks at 2θ values of 38.10º, 44.30 º, 64.45 º, 77.39 º, and 81.49 º respectively. These diffraction peaks matched well with the standard diffraction data (ICDD Card No. 00-004-0783). The average crystallite size of the TpF-AgNPs estimated from FWHM (Table 1) of the diffraction peaks calculated using Debye-Scherrer's equation, $D = K\lambda/\beta\cos\theta$ was found to be 24.21 nm.

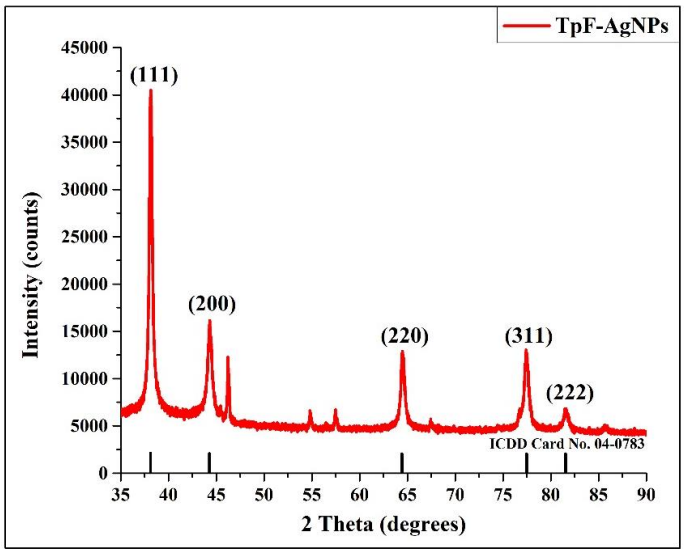

Figure 4 X-Ray Diffraction pattern of *T. paniculata* fruit extract mediated AgNPs

Table 1 XRD profile of *T. paniculata* fruit extract mediated AgNPs

Position 2θ (º)	Height (counts)	FWHM (º)	d-spacing (Å)	Planes (hkl)	Particle Size (nm)
38.1097	1476.9	0.3231	2.3594	(111)	27.16
44.3021	406.6	0.5062	2.0429	(200)	17.69
64.4526	371.5	0.3616	1.4444	(220)	27.12
77.3942	387	0.4083	1.2320	(311)	26.03
81.4959	96.6	0.4744	1.1801	(222)	23.08
Average crystallite size					**24.21**

FWHM – Full Width Half Maximum

DLS Particle Size and Zeta Potential Analysis

DLS particle size analyzer is an analytical tool used to measure particle size and surface charge on the nanoparticles. From figure 5(A), the mean particle size was found to be 72.8 nm and Z-average particle size was 40.2 nm with a polydispersity index of 0.448 and the zeta potential value of -53.9 mV (Figure 5B) which indicated excellent stability of the nanoparticles.

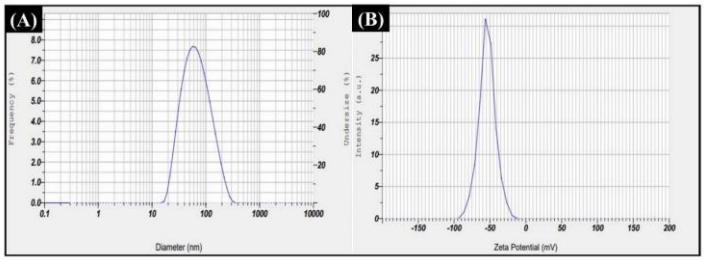

Figure 5 (A) Particle size and (B) Zeta potential of TpF-AgNPs

AFM Analysis

The surface topography of the TpF-AgNPs was analyzed using the AFM technique. The images (Figure 6) depict the polydispersed and spherical shape of nanoparticles with sizes ranging from 30 to 85 nm.

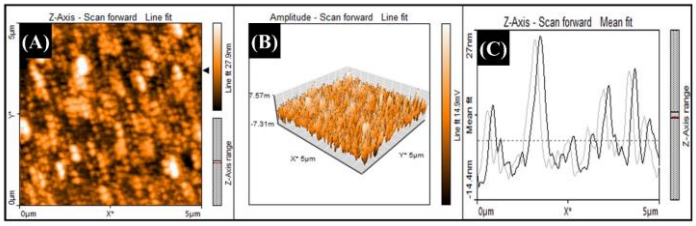

Figure 6 AFM images of TpF-AgNPs (A) 2-Dimensional, (B) 3-Dimensional and (C) Particle size distribution

HR-TEM with SAED Analysis

HR-TEM explores the detailed microscopic structure of the AgNPs. The TEM image of TpF-AgNPs is shown in Figure 7(A) which depicts the spherical shape and polydispersity of the nanoparticles. A histogram of particle size distribution represents that the TpF-AgNPs varied in size between 5 and 50 nm with an average particle size of 26.03 ± 7.54, n = 98 (Figure 7B). The HR-TEM image (Figure 7C) shows the lattice fringe with a distance of 2.36 Å (0.23 nm). The SAED pattern shows five bright circular rings (Figure 7D) assigned to (111), (200), (220), (311), and (222) which are the characteristic reflections of face-centered cubic crystalline silver that correlates with the XRD pattern.

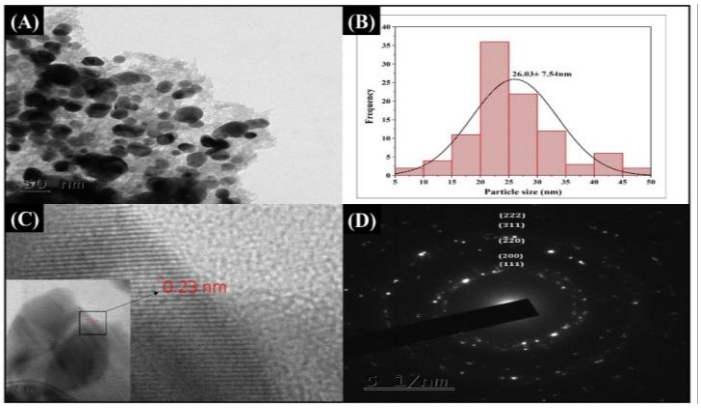

Figure 7 HR-TEM and SAED pattern of TpF-AgNPs

DPPH Free Radical Scavenging Assay

The DPPH free radical scavenging assay determines the antioxidant capacity of extracts or AgNPs to scavenge free radicals by a change in colour from purple to yellow or colourless. As shown in figure 8, both TpF-AgNPs and fruit extract showed increased activity in a dose-dependent manner with maximum % scavenging of 71.72 ± 0.51% for TpF-AgNPs and 78.30 ± 0.31% for fruit extract recorded at their highest concentration (100 µg/mL). The standard drug Ascorbic acid showed 96.88 ± 0.37% scavenging at a concentration of 100 µg/mL. The IC50 values obtained for TpF-AgNPs, fruit extract and standard were 71.02, 68.59 and 40.99 µg/mL (Table 2) respectively.

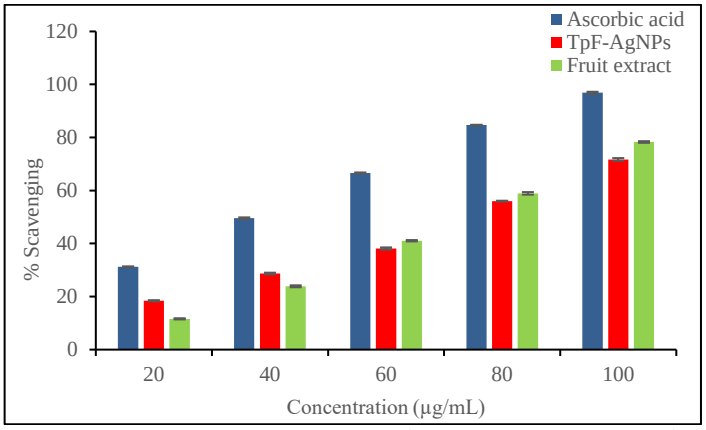

Figure 8 DPPH radical scavenging activity of TpF-AgNPs compared with fruit extract and standard ascorbic acid

Table 2 % Scavenging and IC50 values of TpF-AgNPs, fruit extract and Ascorbic acid for DPPH free radical scavenging assay

Sl. No.	Concentration (µg/mL)	% Scavenging		
		Ascorbic acid	TpF-AgNPs	Fruit extract
1	20	31.28 ± 0.11^{Ea}	18.43 ± 0.21^{Eb}	11.60 ± 0.22^{Ec}
2	40	49.55 ± 0.31^{Da}	28.71 ± 0.30^{Db}	23.88 ± 0.36^{Dc}
3	60	66.59 ± 0.22^{Ca}	38.14 ± 0.39^{Cc}	41.06 ± 0.25^{Cb}
4	80	84.68 ± 0.12^{Ba}	56.04 ± 0.11^{Bc}	58.93 ± 0.48^{Bb}
5	100	96.88 ± 0.37^{Aa}	71.72 ± 0.51^{Ac}	78.30 ± 0.31^{Ab}
	IC50	**40.99**	**71.02**	**68.59**

Data expressed as mean ± standard deviation (n = 3). Different superscript capital letters within a column and different superscript small letters within a row denote significant differences ($p < 0.05$).

BSA Protein Anti-denaturation Assay

The BSA protein anti-denaturation assay determines the ability of extracts or AgNPs in inhibiting the protein denaturation which is the main cause for inflammation. Here the decrease in absorbance with increasing concentration showed the % inhibition of protein denaturation. The results (Figure 9) showed an increase in inhibition of protein denaturation in a dose-dependent manner with maximum % inhibition of 85.88 ± 1.09% for TpF-AgNPs and 70.21 ± 1.10% for fruit extract recorded at their highest concentration (500 µg/mL). The Standard drug Diclofenac Sodium showed 97.16 ± 1.14% inhibition of protein denaturation at a concentration of 500 µg/mL. The IC50 values obtained for TpF-AgNPs, fruit extract and standard were 201.88, 320.22 and 121.99 µg/mL (Table 3) respectively.

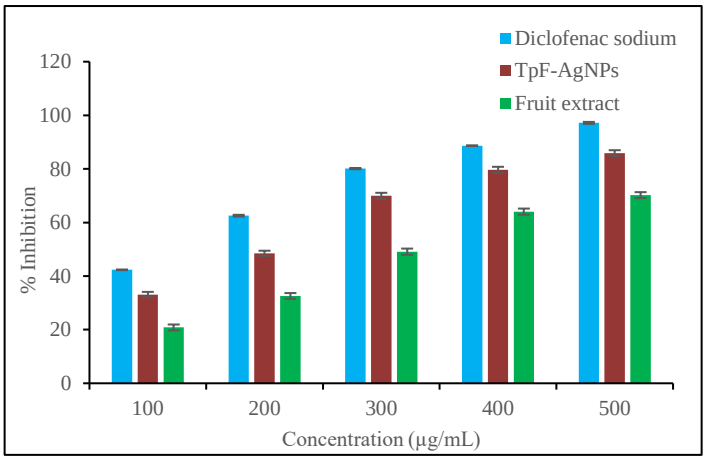

Figure 9 BSA protein anti-denaturation activity of TpF-AgNPs compared with fruit extract and standard diclofenac sodium

Table 3 % Inhibition and IC50 values of TpF-AgNPs, fruit extract and Diclofenac sodium for BSA anti-denaturation assay

Sl. No.	Concentration (µg/mL)	% Inhibition of protein denaturation		
		Diclofenac sodium	TpF-AgNPs	Fruit extract
1	100	42.33 ± 1.05^{Ea}	33.10 ± 1.00^{Eb}	20.84 ± 1.09^{Ec}
2	200	62.54 ± 1.02^{Da}	48.50 ± 0.96^{Db}	32.60 ± 1.06^{Dc}
3	300	80.11 ± 1.08^{Ca}	69.94 ± 1.13^{Cb}	49.10 ± 1.15^{Cc}
4	400	88.67 ± 1.04^{Ba}	79.66 ± 1.12^{Bb}	64.06 ± 1.13^{Bc}
5	500	97.16 ± 1.14^{Aa}	85.88 ± 1.09^{Ab}	70.21 ± 1.10^{Ac}
	IC50	**121.99**	**201.88**	**320.22**

Data expressed as mean ± standard deviation (n = 3). Different superscript capital letters within a column and different superscript small letters within a row denote significant differences ($p < 0.05$).

DISCUSSION

The present study reports the successful synthesis of silver nanoparticles using aqueous fruit extract of *Terminalia paniculata* Roth under direct sunlight and its efficient antioxidant and anti-inflammatory activity. Visual transition in colour from pale-yellow to reddish-brown indicates the formation of silver nanoparticles confirmed by UV-Vis Spectroscopy. A similar colour inference was observed in studies on AgNPs synthesis using leaf extract of *Polygonatum graminifolium* **(Rawat *et al.*, 2020)** and *Ocimum sanctum* **(Brahmachari *et al.*, 2014)**. The colour change is mainly due to the collective oscillation of free electrons present on the surface of metal nanoparticles. This is as a result of interaction with the electric field component of the incident light in a phenomenon called Surface Plasmon Resonance (SPR). The SPR peak of AgNPs falls in the visible light region of the electromagnetic spectrum in the range of 400-450 nm **(Chutrakulwong *et al.*, 2020)**.

From the UV-Vis spectral results, it can be seen that pH affects the rate of formation of nanoparticles. In this, a mild shift occurred in the SPR band from 420 nm to 411 nm with a change in pH from 4.3 to 8 and also a change in broader peak to a sharper one with increased absorbance. It is observed that in alkaline conditions, the increase in negatively charged hydroxide ions (OH^-) leads to a fast reduction of Ag^+ to Ag^0 and nucleation, resulting in the formation of large quantities of small-sized nanoparticles. While in acidic conditions, the nucleation rate is slower due to electrostatic repulsion of anions resulting in large-sized nanoparticles **(Chutrakulwong *et al.*, 2020; Edison and Sethuraman, 2012)**. According to Mie's theory, the absorption spectra of spherical nanoparticles generally shows a single SPR band whereas two or more SPR bands indicate variation in the shape of nanoparticles **(Kumar *et al.*, 2017)**. In the present work, a single SPR band was produced indicating the spherical shape of nanoparticles, also confirmed by HR-TEM analysis.

The effect of sunlight on nanoparticle formation with instant colour change indicated that the reaction was completely photocatalytic with no extra heating or stirring. Similar results have been reported in the synthesis of AgNPs using aqueous *Physalis angulata* leaf extract **(Kumar *et al.*, 2017)**. With an increase in exposure time, the colour intensity of the reaction mixture increased up to 5 mins but with further exposure, the solution showed a slight greyish tinge. Studies on AgNPs synthesis using durian rind extract have shown that though a long time of exposure to sunlight enhances the reduction process but leads to aggregation resulting in the formation of large-sized nanoparticles **(Chutrakulwong *et al.*, 2020)**. It is also noticed that synthesis of AgNPs occurs even at room temperature but the time required to complete the reaction was several times more compared to sunlight exposure. Dark conditions did not favor the formation of AgNPs. Among the three possible conditions mentioned, AgNPs were formed in both sunlight and at room temp, but the time taken for the reaction was less under direct sunlight (< 3 mins) compared to room temp (20 mins). So, the sunlight-driven synthesis of silver nanoparticles is quicker considering the time factor.

The FTIR spectra showed major shifting of peaks and reduction of peak intensity from 3399 cm^{-1} to 3424 cm^{-1} and 1055 cm^{-1} to 1020 cm^{-1} which provides clear evidence of involvement of the phytochemicals from the fruit extract in AgNPs formation. This indicates that the hydroxyl (-OH) and amine (-NH) functional groups were mainly responsible for reduction and capping of silver nanoparticles. These functional groups pertain to phytochemicals such as phenolics and aminoacids. The results are consistent with previous report on phytochemical studies which revealed the presence of alkaloids, anthocyanins, coumarins, phenols, and saponins in aqueous fruit extract of *T. paniculata* **(Rajashekhar *et al.*, 2016)**.

X-ray diffraction studies showed five distinct Braggs diffraction peaks which correspond to (111), (200), (220), (311) and (222) planes of Face Centered Cubic (FCC) phase of metallic silver confirmed by comparing with the standard pattern. This clearly shows that the AgNPs formed using aqueous fruit extract of *T. paniculata* were crystalline in nature. These results are in good agreement with earlier findings **(Sumitha *et al.*, 2019b)**. In addition to these peaks, some unassigned peaks were also observed suggesting the crystallization of bio-inorganic phase on the surface of silver nanoparticles **(Ponarulselvam *et al.* 2012)**.

The particle size of 40.2 nm obtained through DLS substantiates with TEM data. Such results were obtained in previous reports where the average size was 39.41 nm for AgNPs synthesized using bark extract of *Amentotaxus assamica* **(Bharali *et al*., 2019)**. Polydispersity Index (PDI) shows the spread of particle size distribution with the value ranging from 0.1 to 1. PDI with a value less than 0.1 indicates monodispersity, whereas more than 0.1 implies polydispersity **(Raval *et al*., 2019)**. The obtained PDI value of 0.448 shows the polydisperse nature of TpF-AgNPs.

Zeta potential is an indicator of stability of nanoparticles based on the surface charge. As per the literature, the value of zeta potential higher than +30 or lower than -30 is considered highly stable in dispersion medium **(Erdogan *et al*., 2019)**. In the present study, the zeta potential of -53.9 mV indicates excellent stability and the negative ions on the surface of the particles implies a strong repulsive force that reduces the possibility of aggregation and enhances the stability of nanoparticles **(Badmus *et al*., 2020)**.

From the AFM studies, it can be predicted that the TpF-AgNPs were more or less spherical in shape with random distribution. The particle size evaluated from AFM images was comparatively larger than that obtained from XRD, DLS, and TEM analysis. This could be due to the aggregation of AgNPs during the preparation of the slide for analytical examination **(Alahmad *et al*., 2013)**. Our results correlate with the previous studies, where the AgNPs synthesized using soyabean seed extract were spherical and their size ranged from 60-80 nm **(Sandeep and Biradarpatil, 2018)**.

TEM images show polydisperse spherical TpF-AgNPs of different sizes with less agglomeration. The lattice fringes in the HR-TEM image and bright circular rings from the SAED pattern further confirmed the crystalline nature of TpF-AgNPs. This is in accordance with the results obtained by **Alshehri and Malik (2020)**, where the size ranged from 5 to 40 nm of AgNPs synthesized using *Matricaria chamomilla*.

DPPH radical scavenging activity is a very simple and inexpensive method to determine the antioxidant potential of the compounds. DPPH (2,2-diphenyl-1-picrylhydrazyl) is a stable free radical with an odd electron on the nitrogen atom, producing deep violet colour in methanol **(Blois, 1958)**. It can accept an electron or hydrogen atom from the donor. On receiving, the odd electron is reduced to corresponding hydrazine with loss of colour **(Contreras-Guzman and Strong, 1982)**. This degree of discolouration is made use to assess the antioxidant capacity. In the present findings, TpF-AgNPs showed significant ($p < 0.05$) activity at lower concentrations 20 and 40 µg/mL compared to fruit extract. But with increasing concentration, extract showed increased activity. This could be due to the greater availability of reducing groups in the extract than on the surface of TpF-AgNPs. It clearly shows that the antioxidant potential of TpF-AgNPs was due to the phytochemicals capped on the surface of AgNPs which is evident from FTIR analysis. Similar results were observed with AgNPs synthesized from *Nigella arvensis* leaf extract **(Chahardoli *et al*., 2018)**.

It is known that protein denaturation is a well-documented cause of inflammation **(Opie, 1962)**. The anti-inflammatory activity was assessed via the % inhibition of heat-induced protein denaturation. In the present work, TpF-AgNPs exhibited significantly ($p < 0.05$) higher activity compared to the fruit extract. Such results were also reported by **Prabhakaran and Mani (2019)**. Although TpF-AgNPs showed moderate antioxidant activity, its effect on inhibition of protein denaturation was almost near to the standard. The exact mechanism of interaction of nanoparticles in stabilizing the protein can be understood with further docking studies.

CONCLUSION

In the present investigation, a very efficient method to synthesize silver nanoparticles (AgNPs) using aqueous fruit extract of *Terminalia paniculata* Roth under direct sunlight is reported. The results show that sunlight favors the rapid fabrication of AgNPs compared to other temperature-mediated synthesis by reducing the time factor. The spectroscopic and microscopic studies reveal that TpF-AgNPs were spherical, stable, crystalline with particle size ranging from 5-50 nm. FTIR spectra shows the involvement of phytochemicals in the reduction, capping, and stabilization of TpF-AgNPs, which exhibited significant antioxidant and anti-inflammatory activities.

Acknowledgements: The authors are thankful to the Chairman, P.G. Department of Studies in Botany, Karnatak University, Dharwad for Laboratory facilities. The first author is thankful to DST-KSTePS (DST/KSTePS/Ph.D. Fellowship/LIF-05:2019-20) and University Research Studentship (KUD/SCH/URS/2019/346) for providing financial assistance in the form of fellowship. We also acknowledge USIC (University Scientific Instrumentation Centre), SAIF (Sophisticated Analytical Instrument Facility), DST-PURSE Phase-II programme, Karnatak University and KIDNAR (Karnataka Institute for DNA Research), Pavate Nagar, Dharwad for providing all the necessary facilities required to carry out the research work. We also thank DST-SAIF, STIC Cochin, Kerala for helping us with HR-TEM analysis.

REFERENCES

Abo-Elmagd, R. A., Hussein, M. H., Hamouda, R. A., Shalan, A. E., & Abdelrazak, A. (2020). Statistical optimization of photo-induced biofabrication of silver nanoparticles using the cell extract of *Oscillatoria limnetica*: insight on characterization and antioxidant potentiality. *RSC Advances*, 10(72), 44232–44246. https://doi:10.1039/d0ra08206f

Ahmed, S. & Ikram, S. (2015). Silver Nanoparticles: One pot green synthesis using *Terminalia arjuna* extract for biological application. *Journal of Nanomedicine & Nanotechnology*, 06(04). http://dx.doi.org/10.4172/2157-7439.1000309.

Alahmad, A., Eleoui, M., Falah, A., Alghoraibi, I. (2013). Preparation of colloidal silver nanoparticles and structural characterization. *Physical Science Research International*, 1(4):89-96.

Alshehri, A. A., & Malik, M. A. (2020). Phytomediated photo-induced green synthesis of silver nanoparticles using *Matricaria chamomilla* L. and its catalytic activity against Rhodamine B. *Biomolecules*, 10(12), 1604. http://dx.doi:10.3390/biom10121604

Aswathi, P., & Ernest Thoppil, J. (2020). Assessment of antioxidant potential and antigenotoxicity analysis through hydrogen peroxide-induced oxidative stress in *Terminalia paniculata* Roth. *Asian Journal of Pharmaceutical and Clinical Research*, 108–112. https://doi:10.22159/ajpcr.2020.v13i8.38123

Aware, C., Patil, R., Gaikwad, S., Yadav, S., Bapat, V., & Jadhav, J. (2017). Evaluation of L-dopa, proximate composition with *in vitro* anti-inflammatory and antioxidant activity of *Mucuna macrocarpa* beans: A future drug for Parkinson treatment. *Asian Pacific Journal of Tropical Biomedicine*, 7(12), 1097–1106. https://doi:10.1016/j.apjtb.2017.10.012

Badmus, J. A., Oyemomi, S. A., Adedosu, O. T., Yekeen, T. A., Azeez, M. A., Adebayo, E. A., … Marnewick, J. L. (2020). Photo-assisted bio-fabrication of silver nanoparticles using *Annona muricata* leaf extract: exploring the antioxidant, anti-diabetic, antimicrobial, and cytotoxic activities. *Heliyon*, 6(11), e05413. https://doi:10.1016/j.heliyon.2020.e05413

Bharali, P., Das, S., Bhandari, N., Das, A. K., & Kalta, M. C. (2019). Sunlight induced biosynthesis of silver nanoparticle from the bark extract of *Amentotaxus assamica* D.K. Ferguson and its antibacterial activity against *Escherichia coli* and *Staphylococcus aureus*. *IET Nanobiotechnology*, 13(1), 18–22. https://doi:10.1049/iet-nbt.2018.5036

Blois, M. S. (1958). Antioxidant determinations by the use of a stable free radical. *Nature*, 181(4617), 1199–1200. https://doi:10.1038/1811199a0

Botterweck, A. A M., Verhagen, H., Goldbohm, R.., Kleinjans, J., & van den Brandt, P. (2000). Intake of butylated hydroxyanisole and butylated hydroxytoluene and stomach cancer risk: results from analyses in the Netherlands Cohort Study. *Food and Chemical Toxicology*, 38(7), 599–605. https://doi:10.1016/s0278-6915(00)00042-9

Brahmachari, G., Sarkar, S., Ghosh, R., Barman, S., Mandal, N. C., Jash, S. K., … Roy, R. (2014). Sunlight-induced rapid and efficient biogenic synthesis of silver nanoparticles using aqueous leaf extract of *Ocimum sanctum* Linn. with enhanced antibacterial activity. *Organic and Medicinal Chemistry Letters*, 4(1). https://doi:10.1186/s13588-014-0018-6

Cai, Y., Luo, Q., Sun, M., & Corke, H. (2004). Antioxidant activity and phenolic compounds of 112 traditional Chinese medicinal plants associated with anticancer. *Life Sciences*, 74(17), 2157–2184. https://doi:10.1016/j.lfs.2003.09.047

Chahardoli, A., Karimi, N., & Fattahi, A. (2018). *Nigella arvensis* leaf extract mediated green synthesis of silver nanoparticles: Their characteristic properties and biological efficacy. *Advanced Powder Technology*, 29(1), 202–210. https://doi:10.1016/j.apt.2017.11.003

Chandra, S., Chatterjee, P., Dey, P., & Bhattacharya, S. (2012). Evaluation of *in vitro* anti-inflammatory activity of coffee against the denaturation of protein. *Asian Pacific Journal of Tropical Biomedicine*, 2(1), S178–S180. https://doi:10.1016/s2221-1691(12)60154-3

Chaudhuri, S. K., & Malodia, L. (2017). Biosynthesis of zinc oxide nanoparticles using leaf extract of *Calotropis gigantea*: characterization and its evaluation on tree seedling growth in nursery stage. *Applied Nanoscience*, 7, 501-512. https://doi.org/10.1007/s13204-017-0586-7

Chutrakulwong, F., Thamaphat, K., & Limsuwan, P. (2020). Photo-irradiation induced green synthesis of highly stable silver nanoparticles using durian rind biomass: Effects of light intensity, exposure time and pH on silver nanoparticles formation. *Journal of Physics Communications*, 4(9), 095015. https://doi:10.1088/2399-6528/abb4b5

Contreras-Guzmán, E. S., & Strong, F. C. (1982). Determination of tocopherols (Vitamin E) by reduction of cupric ion. *Journal of AOAC International*, 65(5), 1215–1221. https://doi:10.1093/jaoac/65.5.1215

Edison, T. J. I., & Sethuraman, M. G. (2012). Instant green synthesis of silver nanoparticles using *Terminalia chebula* fruit extract and evaluation of their catalytic activity on reduction of methylene blue. *Process Biochemistry*, 47(9), 1351–1357. https://doi:10.1016/j.procbio.2012.04.025

Eloff, J. N., Katerere, D. R., & McGaw, L. J. (2008). The biological activity and chemistry of the southern African Combretaceae. *Journal of Ethnopharmacology*, 119(3), 686–699. https://doi:10.1016/j.jep.2008.07.051

Erdogan, O., Abbak, M., Demirbolat, G. M., Birtekocak, F., Aksel, M., Pasa, S., & Cevik, O. (2019). Green synthesis of silver nanoparticles via *Cynara scolymus* leaf extracts: The characterization, anticancer potential with photodynamic therapy in MCF7 cells. *PLOS ONE*, 14(6), e0216496. https://doi:10.1371/journal.pone.0216496

Grant, N. H., Alburn, H. E., & Kryzanauskas, C. (1970). Stabilization of serum albumin by anti-inflammatory drugs. *Biochemical Pharmacology*, 19(3), 715–722. https://doi:10.1016/0006-2952(70)90234-0

Hashemi, S., Asrar, Z., Pourseyedi, S., & Nadernejad, N. (2016). Plant-mediated synthesis of zinc oxide nano-particles and their effect on growth, lipid peroxidation and hydrogen peroxide contents in soybean. *Indian Journal of Plant Physiology*, 21(3), 312–317. https://doi.org/10.1007/s40502-016-0242-3

Herlekar, M., Barve, S., & Kumar, R. (2014). Plant-mediated green synthesis of iron nanoparticles. *Journal of Nanoparticles*, 2014, 1–9. https://doi.org/10.1155/2014/140614

Horikoshi, S., & Serpone, N. (2013). Introduction to nanoparticles. *Microwaves in Nanoparticle Synthesis*, 1–24. https://doi.org/10.1002/9783527648122

Jose, V. Raphel, L., Aiswariya, K. S. and Mathew, P.(2021). Green synthesis of silver nanoparticles using *Annona squamosa* L. seed extract: characterization, photocatalytic and biological activity assay. *Bioprocess and Biosystems Engineering*, 44(9), pp.1819–1829. http://dx.doi.org/10.1007/s00449-021-02562-2.

Kumar, V., Singh, D. K., Mohan, S., Gundampati, R. K., & Hasan, S. H. (2017). Photoinduced green synthesis of silver nanoparticles using aqueous extract of *Physalis angulata* and its antibacterial and antioxidant activity. *Journal of Environmental Chemical Engineering*, 5(1), 744–756. https://doi:10.1016/j.jece.2016.12.055

Mohamed El-Rafie, H., & Abdel-Aziz Hamed, M. (2014). Antioxidant and anti-inflammatory activities of silver nanoparticles biosynthesized from aqueous leaves extracts of four *Terminalia* species. *Advances in Natural Sciences: Nanoscience and Nanotechnology*, 5(3), 035008. https://doi:10.1088/2043-6262/5/3/035008

Mohan Kumar, K., Sinha, M., Mandal, B. K., Ghosh, A. R., Siva Kumar, K., & Sreedhara Reddy, P. (2012). Green synthesis of silver nanoparticles using *Terminalia chebula* extract at room temperature and their antimicrobial studies. *Spectrochimica Acta Part A: Molecular and Biomolecular Spectroscopy*, 91, 228–233. https://doi:10.1016/j.saa.2012.02.001

Narayana, J. & Chitra, V. (2018). *In vitro* anti-inflammatory activity of *Garcinia hanburyi* extract. *Journal of Pharmacy Research*, 12(4):571–6.

Ng, S., Lasekan, O., Muhammad, K., Sulaiman, R., & Hussain, N. (2014). Effect of roasting conditions on color development and Fourier transform infrared spectroscopy (FTIR-ATR) analysis of Malaysian-grown tropical almond nuts (*Terminalia catappa* L.). *Chemistry Central Journal*, 8(1). https://doi:10.1186/s13065-014-0055-2

Opie, E. L. (1962). On the relation of necrosis and inflammation to denaturation of proteins. *Journal of Experimental Medicine*, 115(3), 597–608. https://doi:10.1084/jem.115.3.597

Patil, S., Chaudhari, G., Paradeshi, J., Mahajan, R., & Chaudhari, B. L. (2017). Instant green synthesis of silver-based herbo-metallic colloidal nanosuspension in *Terminalia bellirica* fruit aqueous extract for catalytic and antibacterial applications. *3 Biotech*, 7(1). https://doi:10.1007/s13205-016-0589-1

Ponarulselvam, S., Panneerselvam, C., Murugan, K., Aarthi, N., Kalimuthu, K., & Thangamani, S. (2012). Synthesis of silver nanoparticles using leaves of *Catharanthus roseus* Linn. G. Don and their antiplasmodial activities. *Asian Pacific Journal of Tropical Biomedicine*, 2(7), 574–580. https://doi:10.1016/s2221-1691(12)60100-2

Prabakaran, A. S. & Mani, N. (2019). Anti-inflammatory activity of silver nanoparticles synthesized from *Eichhornia crassipes*: An *in vitro* study. *Journal of Pharmacognosy and Phytochemistry*, 8(4):2556-2558.

Rajasekhar, K, Venkata Raju, RR. (2016). Phytochemical, antioxidant and antimicrobial studies of *Terminalia paniculata*- a potential medicinal plant. *International Journal of Pharmacognosy and Phytochemical Research*, 8(1):14–7.

Raval, N., Maheshwari, R., Kalyane, D., Youngren-Ortiz, S. R., Chougule, M. B., & Tekade, R. K. (2019). Importance of physicochemical characterization of nanoparticles in pharmaceutical product development. *Basic Fundamentals of Drug Delivery*, 369–400. https://doi:10.1016/b978-0-12-817909-3.00010-8

Ravipati, A. S., Zhang, L., Koyyalamudi, S. R., Jeong, S. C., Reddy, N., Bartlett, J., … Vysetti, B. (2012). Antioxidant and anti-inflammatory activities of selected Chinese medicinal plants and their relation with antioxidant content. *BMC Complementary and Alternative Medicine*, 12(1). https://doi:10.1186/1472-6882-12-173

Ray, P. D., Huang, B.W., & Tsuji, Y. (2012). Reactive oxygen species (ROS) homeostasis and redox regulation in cellular signaling. *Cellular Signalling*, 24(5), 981–990. https://doi:10.1016/j.cellsig.2012.01.008

Ríos, J. L., & Recio, M. C. (2005). Medicinal plants and antimicrobial activity. *Journal of Ethnopharmacology*, 100(1-2), 80–84. https://doi.org/10.1016/j.jep.2005.04.025

Sagadevan, S., Vennila, S., Singh, P., Lett, J. A., Johan, M. R., Marlinda, A. R., … Lakshmipathy, M. (2019). Facile synthesis of silver nanoparticles using *Averrhoa bilimbi* L and Plum extracts and investigation on the synergistic bioactivity using *in vitro* models. *Green Processing and Synthesis*, 8(1), 873–884. https://doi:10.1515/gps-2019-0058

Sandeep, D. & Biradarpatil, N. K. (2018). Biosynthesis of silver nanoparticles using soybean seed extract. *Journal of Pharmacognosy and Phytochemistry*, 7(4):2676-2680

Singh, C., Kumar, J., Kumar, P., Chauhan, B. S., Tiwari, K. N., Mishra, S. K., … Singh, J. (2019). Green synthesis of silver nanoparticles using aqueous leaf extract of *Premna integrifolia* (L.) rich in polyphenols and evaluation of their antioxidant, antibacterial and cytotoxic activity. *Biotechnology & Biotechnological Equipment*, 33(1), 359–371. https://doi:10.1080/13102818.2019.1577699

Sivamaruthi, B. S., Ramkumar, V. S., Archunan, G., Chaiyasut, C., & Suganthy, N. (2019). Biogenic synthesis of silver palladium bimetallic nanoparticles from fruit extract of *Terminalia chebula* – *In vitro* evaluation of anticancer and antimicrobial activity. *Journal of Drug Delivery Science and Technology*, 51, 139–151. https://doi:10.1016/j.jddst.2019.02.024

Sooraj, M. P., Nair, A. S., & Vineetha, D. (2021). Sunlight-mediated green synthesis of silver nanoparticles using *Sida retusa* leaf extract and assessment of its antimicrobial and catalytic activities. *Chemical Papers*, 75(1), 351–363. https://doi:10.1007/s11696-020-01304-0

Sumitha, S., Vasanthi, S., Shalini, S., Chinni, S. V., Gopinath, S. C. B., Anbu, P., … Ravichandran, V. (2018a). Phyto-mediated photo catalysed green synthesis of silver nanoparticles using *Durio zibethinus* seed extract: Antimicrobial and cytotoxic activity and photocatalytic applications. *Molecules*, 23(12), 3311. https://doi:10.3390/molecules23123311

Sumitha, S., Vasanthi, S., Shalini, S., Chinni, S., B. Gopinath, S., … Ravichandran, V. (2019b). *Durio zibethinus* rind extract mediated green synthesis of silver nanoparticles: Characterization and biomedical applications. *Pharmacognosy Magazine*, 15(60), 52. https://doi:10.4103/pm.pm_400_18

Talwar, S., Nandakumar, K., Nayak, P. G., Bansal, P., Mudgal, J., Mor, V., … Lobo, R. (2011). Anti-inflammatory activity of *Terminalia paniculata* bark extract against acute and chronic inflammation in rats. *Journal of Ethnopharmacology*, 134(2), 323–328. https://doi:10.1016/j.jep.2010.12.015

Tripathi, K. (2008). Essentials of medical pharmacology. 6th ed. New Dehli: Jaypee Brothers Medical publishers (P) Ltd. https://doi:10.5005/jp/books/10282

Valko, M., Leibfritz, D., Moncol, J., Cronin, M. T. D., Mazur, M., & Telser, J. (2007). Free radicals and antioxidants in normal physiological functions and human disease. The *International Journal of Biochemistry & Cell Biology*, 39(1), 44–84. https://doi:10.1016/j.biocel.2006.07.001

Venkatasubbaiah, R., Jha, P. K., & Sanjay, K. R. (2021). *Centella asiatica* crop residue fabricated silver nanoparticles as potent antioxidant agents in photo-catalytic degradation of hazardous dyes. *Chemical Engineering Communications*, 209(7), 938–956. https://doi:10.1080/00986445.2021.1931146